

# Preparation, Mechanism Analysis, and Physiological Signal Monitoring Applications of a Flexible Sensing System Integrated with InSnZnO TFTs

Mei Yang\*, Wei Huang\*, Man Chun Tseng\*\*, Fion Sze Yan Yeung\*\*, Hoi Sing Kwok\*\*, Rongsheng Chen\*, \*\*

\*School of Microelectronics, South China University of Technology, Guangzhou, China

\*\* State Key Laboratory of Advanced Displays and Optoelectronics Technologies, Department of Electronic and Computer Engineering, The Hong Kong University of Science and Technology, Hong Kong, China

## Abstract

*This study presents a flexible piezoelectric sensor combining electrospun PVDF, ZnO nanorods, and MXene layers (PZM), integrated with ITZO TFTs. The sensor achieves high sensitivity, rapid response, and long-term stability, enabling applications in physiological signal detection and wearable devices for human-computer interaction and soft robotics.*

## Author Keywords

Piezoelectric sensor; InSnZnO Thin-film transistors (ITZO TFTs); System integration research; Physiological signal monitoring.

## 1. Introduction

With the rapid advancements in electronic devices and intelligent systems, flexible pressure sensors have gained significant research interest, particularly in applications like wearable medical equipment, interactive touch screens, and humanoids [1]. Among these, piezoelectric sensors are highly valued for their self-powering capabilities, enabling them to generate voltage signals without external power [2]. These sensors also offer mechanical stability, structural simplicity, low signal crosstalk, and high sensitivity, driving substantial advancements in their development.

Piezoelectric materials, classified into organic and inorganic types, play a crucial role in sensor applications. Organic materials, such as PVDF, are appreciated for their flexibility but often have limited piezoelectric properties. Inorganic materials, including lead zirconate titanate (PZT) and zinc oxide (ZnO), exhibit superior piezoelectric performance but face challenges like low Curie temperatures and limited stability [3]. PVDF stands out as a semi-crystalline polymer favored in wearable sensors due to its low elastic modulus, corrosion resistance, and electromechanical coupling factors comparable to ceramics. Electrospun PVDF materials offer additional benefits such as softness, adjustable morphology, and simplified manufacturing processes without the need for polarization, making them highly suitable for health monitoring and electronic skin applications [4]. However, pure PVDF sensors generally exhibit lower output voltages, which can be improved by incorporating inorganic nanofillers like ZnO to enhance their piezoelectric performance.

Although PZT offers a higher piezoelectric coefficient, its lead content raises concerns about biological safety, limiting its use in wearable technologies. In contrast, ZnO is a non-toxic alternative with straightforward synthesis methods and abundant raw material availability. Integrating ZnO into PVDF has been shown to improve piezoelectric properties. Recent studies have demonstrated that incorporating MXene further enhances sensor performance. MXene, a graphene-like material with high carrier mobility, acts as a filler that boosts the piezoelectric effect by forming micro-capacitors, increasing charge storage, and establishing a conductive network for faster charge migration [5].

Thin-film transistors (TFTs), particularly those based on indium tin zinc oxide (ITZO), play a pivotal role in integrated circuits for flexible electronics. These transistors amplify and process weak signals from sensor units, making them integral to advanced sensor systems. Combining ITZO TFTs with piezoelectric sensors improves signal amplification, ensuring stable and efficient signal acquisition.

In this study, we developed a flexible PVDF/ZnO@MXene (PZM) piezoelectric sensor through a hybrid fabrication approach combining electrospinning, hydrothermal growth, and spin-coating methods. The integration of PVDF nanofibers with ZnO nanoparticles significantly boosted the sensor's piezoelectric performance. Additionally, MXene enhanced charge storage capacity and facilitated the migration of polarized charges, forming a conductive network that further optimized the device's efficiency. To amplify these capabilities, an ITZO TFT with exceptional electrical characteristics was incorporated into the PZM piezoelectric sensor system. The sensor system can achieve signal amplification and ensure stable signal acquisition over 500 cycles, indicating its potential as a wearable electronic device for personalized identification, human-computer interaction, and soft robot manufacturing in the future.

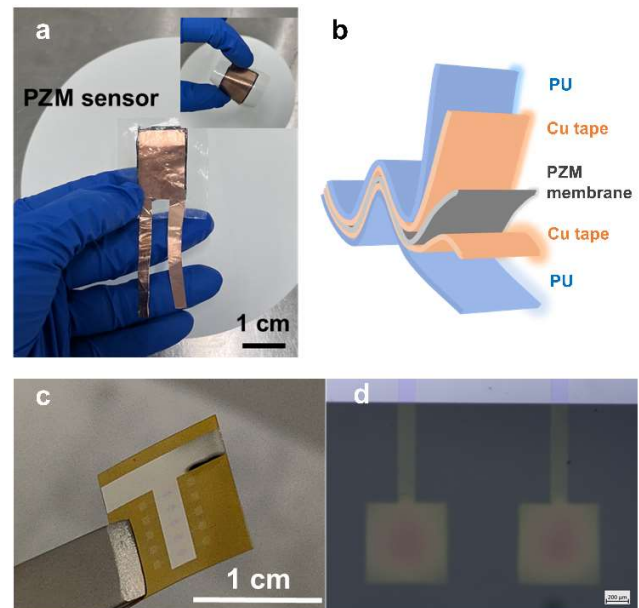


**Figure 1.** (a) Photograph of the PZM piezoelectric sensor. (b) Schematic diagram illustrating the multi-layer structure of the piezoelectric sensor. (c) The physical structure of the ITZO TFT. (d) ITZO TFT morphology under a microscope.

## 2. Experiment

The main experiment consists of following three parts:

### 2.1 Fabrication of PVDF/ZnO@MXene(PZM) Sensor

To fabricate the piezoelectric sensor, a flexible fiber membrane substrate was first produced using electrospinning technology under optimized conditions: an applied voltage of 20 kV, a solute concentration of 15%, and a processing time of 10 h. Following this, a hydrothermal reaction was carried out in a high-pressure reactor at 90°C, with reaction durations set to 3, 5, and 7 h. This process facilitated the preparation of a PVDF composite film (referred to as PZ) that supported the growth of ZnO nanorods. Next, MAX phase precursors were etched following established protocols to obtain a multi-layer MXene aqueous solution. The resulting MXene solution was diluted to a concentration of 5% and spin-coated onto the PZ composite film, forming the PZM active layer with precision, tailored for advanced piezoelectric sensing applications. The PZM fiber membrane, cut to  $1.0 \times 2.0$  cm, was equipped with conductive copper foil as electrodes on both sides. The device was then encapsulated with a protective polyurethane film. A physical image of the sensor is presented in Fig. 1a. Fig. 1b depicts a side view of the device, illustrating its layer-by-layer configuration.

### 2.2 Sensor Testing

The PZM sensor was mounted on a testing platform, with force applied via a universal testing machine and a force gauge. Output voltage signals were recorded through a custom system comprising a commercial force sensor, oscilloscope, DC power supply, and computer terminal.

### 2.3 Integrated Sensing System Research

The PZM piezoelectric sensor was coupled with the gate of an ITZO TFT, creating an integrated device where the TFT amplified and managed electronic signals, while the sensor converted mechanical stimuli into electrical outputs. Fabricated via co-sputtering with a top-gate structure, the TFT's electrical performance was evaluated using the Agilent B1500 semiconductor analyzer. Fig. 1c and Fig. 1d present physical images of the ITZO TFT.

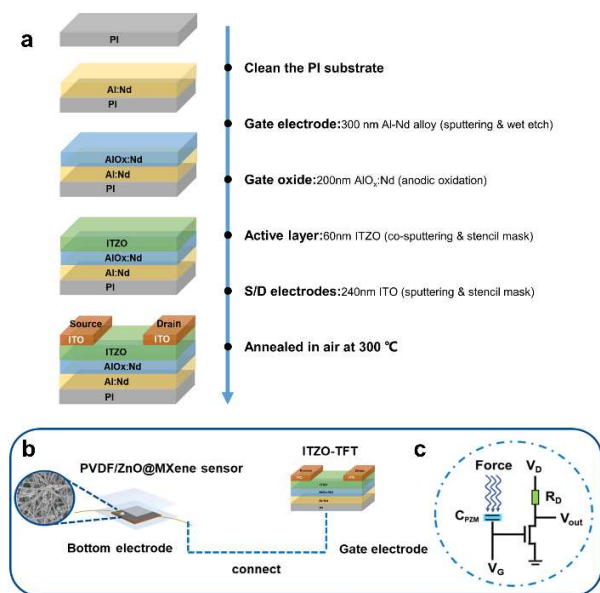


**Figure 2.** (a) ITZO TFT device structure diagram and the specific preparation process. (b) Integrated sensor system diagram. (c) The corresponding circuit diagram.

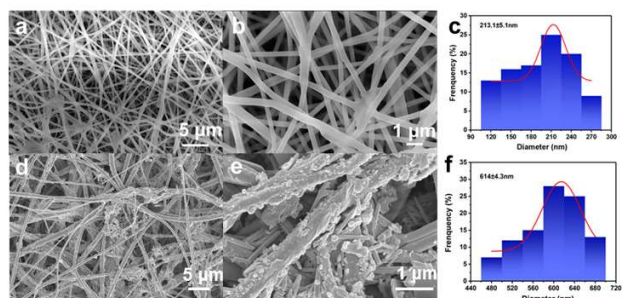


**Figure 3.** (a)~(b) SEM images of pure PVDF. (c) Diameter distribution of pure PVDF film. (d)~(e) SEM images of the PZM film. (f) Diameter distribution of the PZM film.

## 3. Results and discussion

Our investigation focused on the integrated system of sensor devices, where we selected the ITZO TFT for their outstanding electrical performance as the PZM sensor interface. We examined the reliability and stability of the sensor integration system during operation. The TFT uses flexible polyimide (PI) as the substrate, fabricated by the co-sputtering method. The channel width-to-length ratio is  $300 \mu\text{m}/300 \mu\text{m}$ , as illustrated in Fig. 2a. The integrated sensor system and circuit diagrams are presented in Fig. 2b and Fig. 2c. The SEM images in Fig. 3a and Fig. 3b reveal the smooth morphology of pure PVDF fibers, with a diameter distribution of  $213 \pm 5.1$  nm in Fig. 3c. Fig. 3d and Fig. 3e present the irregular protrusions on the surface of the PZM composite membrane fibers, with a diameter distribution of  $614 \pm 4.3$  nm in Fig. 3f.

In the  $\alpha$  phase of PVDF, dipoles are arranged antiparallel, resulting in a non-polar structure with no electrical activity. In contrast, the  $\beta$  phase features aligned dipoles, leading to enhanced electrical activity. The ATR-FTIR spectra in Fig. 4 highlight distinct peaks for PVDF and PZ membranes. The  $\alpha$  phase peaks appear at  $613 \text{ cm}^{-1}$ ,  $763 \text{ cm}^{-1}$ , and  $977 \text{ cm}^{-1}$ , with the  $763 \text{ cm}^{-1}$  peak linked to  $-\text{CH}_2-$  bending vibrations. The  $\beta$  phase is identified by peaks at  $842 \text{ cm}^{-1}$  and  $1278 \text{ cm}^{-1}$ . The relative  $\beta$ -phase content in PVDF and PVDF/ZnO nanofibers was calculated using a standard formula [6],

$$F(\beta) = \frac{A_{\beta}}{\frac{K_{\beta}}{K_{\alpha}} \times A_{\alpha} + A_{\beta}} \times 100\%$$

where  $A_{\alpha}$  and  $A_{\beta}$  are the absorbance at  $763$  and  $842 \text{ cm}^{-1}$ , respectively,  $K_{\alpha}$  and  $K_{\beta}$  are the absorption coefficients of the corresponding wavenumber, and their values are  $7.7 \times 10^4$  and  $6.1 \times 10^4 \text{ cm}^2/\text{mol}$ , respectively. Results showed a significant increase in  $\beta$ -phase content from 66.67% in pure PVDF to 80.57% in PZ nanofibers.

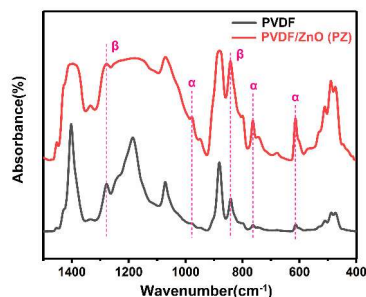


**Figure 4.** FTIR spectra of pure PVDF and PVDF/ZnO.

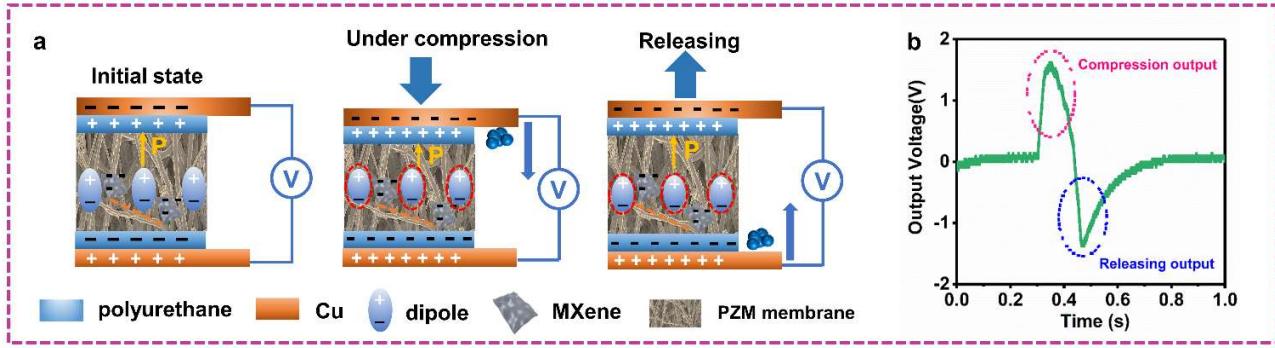


**Figure 5.** (a) Schematic of the sensing mechanism of the PZM piezoelectric device. (b) Corresponding voltage output signal changes.

The operational principle of the PZM piezoelectric device is depicted in Fig. 5. Initially, the electric dipoles within the composite material exhibit a relatively uniform alignment due to self-polarization induced by the built-in electric field. Upon compression, deformation dipoles generate polarization charges on the material's surface, which accumulate to form a piezoelectric potential. To neutralize this potential, free charges migrate toward the electrodes. The heterojunction interface functions as a Schottky barrier, regulating the transport of these charges. Polarization charges are initially trapped on the MXene nanosheets, subsequently migrating rapidly to the electrode surface, thereby enhancing the polarization charge density. When the external stress is released, the accumulated charges flow in the opposite direction.

( $\mu_{sat}$ ), subthreshold swing ( $SS$ ), on-off current ratio ( $I_{on}/I_{off}$ ) and threshold voltage ( $V_{th}$ ) are  $20.52 \text{ cm}^2\text{V}^{-1}\text{s}^{-1}$ ,  $0.074 \text{ V/dec}$ ,  $3.42 \times 10^{10}$ , and  $1.88 \text{ V}$ , respectively. The signal amplification capabilities of the TFT play a pivotal role in enabling accurate processing and interpretation of the electrical signals generated by the piezoelectric sensor within the electronic system. As shown in Fig. 7, the output voltage signal under a light finger touch ( $F = 0.1 \text{ N}$ ) measures  $200 \text{ mV}$  without the integrated TFT. However, with the TFT integration, the signal is amplified to  $1.88 \text{ V}$ . This amplification significantly improves the sensor's ability to detect subtle variations, enhancing its sensitivity and making it more suitable for downstream electronic processing applications.

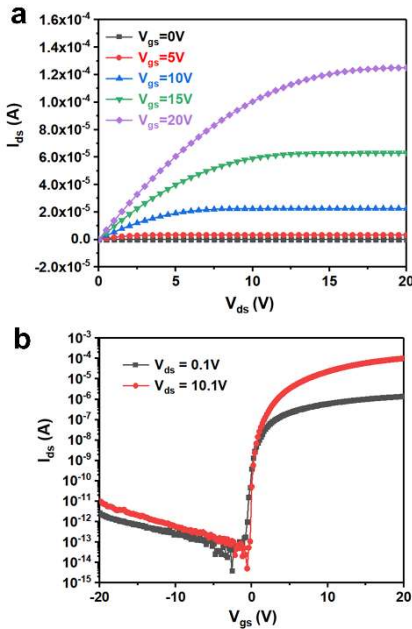


**Figure 6.** (a) The output characteristic curves of the ITZO TFT at different gate voltages. (b) The transfer characteristic curves.

Using a semiconductor analyzer to test the electrical performance parameters of the TFT, the output characteristics curves are depicted in Fig. 6a and the transfer characteristic curves are shown in Fig. 6b. The obtained value of the saturation mobility

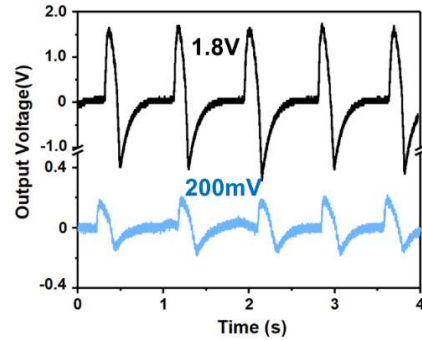


**Figure 7.** The amplification effect of TFT integration on small output signal ( $F=0.1 \text{ N}$ ).

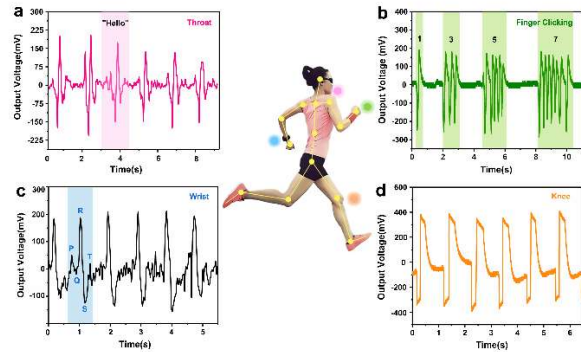


**Figure 8.** The application of PZM sensor in human body dynamic motion monitoring corresponds to the following parts: throat (a), fingers (b), wrist (c), and knee (d).

Fig. 8 illustrate the monitoring capabilities of the PZM sensor for various human activities, including throat vibrations during vocalization, continuous finger tapping, wrist pulse detection, and knee bending, performed by a 26-year-old volunteer. Of particular significance, Fig. 8c captures output signals resembling a typical human electrocardiogram (ECG) waveform, characterized by distinct P, QRS, and T waves, which correspond to atrial excitation, ventricular depolarization, and repolarization processes. This data offers significant potential for cardiovascular disease monitoring and the detection of abnormal stress levels. The established experimental framework lays the foundation for integration with machine learning techniques, enabling advancements in health monitoring, disease prevention, and early warning systems.

Table 1 provides a summary comparing the sensitivity and pressure range of recently developed piezoelectric sensors with the current study.

**Table 1.** Performance comparison between the proposed sensor and reported sensors.

Material	Sensitivity	Pressure range	Ref.
P(VDF-TrFE) nanofibers	60.5 mV N <sup>-1</sup>	0.01~0.06 N	7
PVDF/ZnO nanofibers	0.33 V kPa <sup>-1</sup>	1.8~451 kPa	8
PVDF-PZT nanocomposite	86.58 mV N <sup>-1</sup>	~2.125 N	9
[Hdabco]BF <sub>4</sub> @PVDF composite	640 mV N <sup>-1</sup>	1.6~12.8 kPa	10
ZnO@C/PVDF membrane	0.98 V kPa <sup>-1</sup>	~14.7 N	11
P(VDF-TrFE) fibrous material	29.89 mV N <sup>-1</sup>	0.15~600 kPa	12
Initial PVDF membrane	0.67 V N <sup>-1</sup>	0.01~5 N	This work
PVDF/ZnO@MXene membrane	2.32 V N <sup>-1</sup>	0.01~5 N	This work

#### 4. Conclusion

In conclusion, a flexible piezoelectric sensor with a straightforward fabrication process was successfully developed, demonstrating a rapid response time, high sensitivity, and low energy consumption, making it highly promising for wearable electronic applications. The sensor also showcases versatility by effectively detecting human physiological signals, such as vocal cord vibrations, finger tapping, pulse rates, and knee movements. Furthermore, the integration of the piezoelectric sensor with ITZO TFT exhibits in-situ amplification of weak sensing signals by approximately 10-fold. This integrated system addresses the demands of emerging applications in areas such as human-computer interaction and soft robotics. Moreover, it offers valuable insights into the development of intelligent sensor networks, particularly in the framework of the Internet of Things.

#### 5. Acknowledgements

This work was supported in part by the National Natural Science Foundation of China under Grant 62374060, in part by the Science and Technology Program of Guangzhou under Grant 2024A04J6314, in part by the Fundamental Research Funds for the Central Universities under Grant 2024ZYGXZR097, in part by the TCL Science and Technology Innovation Fund under Grant 20231753, and in part by the State Key Laboratory of Advanced Displays and Optoelectronics Technologies (HKUST).

#### 6. References

- Fastier-Wooller J, Lyons N, Vu T-H, et al. Flexible iron-on sensor embedded in smart sock for gait event detection. *ACS Appl. Mater. Interfaces.*; 2024; 16(1): 1638–1649.
- Dagdeviren C, et al. Conformable amplified lead zirconate titanate sensors with enhanced piezoelectric response for cutaneous pressure monitoring. *Nat. Commun.*; 2014; 5(1).
- Yi Z, et al. High performance bimorph piezoelectric MEMS harvester via bulk PZT thick films on thin beryllium-bronze substrate. *Appl. Phys. Lett.*; 2017; 111(1): 013902.
- Lee S, Bordatchev E, Zeman M. Femtosecond laser micromachining of polyvinylidene fluoride (PVDF) based piezo films. *J. Micromech. Microeng.*; 2008; 18(4): 045011.
- Shahzad F, Alhabeb M, Hatter CB, Anasori B, Hong SM, Koo CM, et al. Electromagnetic interference shielding with 2D transition metal carbides (MXenes). *Science.*; 2016; 353: 1137–1140.
- Cui M, Hou T, Tong J, Xin Y, Zhou X, Liang W. Flexible piezoelectric tactile sensor with cilia-inspired structures based on electrospun PVDF/Fe<sub>3</sub>O<sub>4</sub> nanofibers. *IEEE Sens. J.*; 2022; 22(24): 24430–24438.
- Ren G, Cai F, Li B, Zheng J, Xu C. Flexible pressure sensor based on a poly(VDF-TrFE) nanofiber web. *Macromol. Mater. Eng.*; 2013; 298: 541–546.
- Deng W, et al. Cowpea-structured PVDF/ZnO nanofibers based flexible self-powered piezoelectric bending motion sensor towards remote control of gestures. *Nano Energy*; 2019; 55: 516–525.
- Chamankar N, Khajavi R, Yousefi AA, Rashidi A, Golestanifard F. A flexible piezoelectric pressure sensor based on PVDF nanocomposite fibers doped with PZT particles for energy harvesting applications. *Ceram Int.*; 2020; 46: 19669–19681.
- Deswal S, Khandelwal G, Dahiya R. Molecular ferroelectric based biocompatible flexible piezoelectric pressure sensor. *IEEE Sens Lett.*; 2023; 7(6): 1–4.
- Li X, Ji D, Yu B, Ghosh R, He J, Qin XH, Ramakrishna S. Boosting piezoelectric and triboelectric effects of PVDF nanofiber through carbon-coated piezoelectric nanoparticles for highly sensitive wearable sensors. *Chem. Eng. J.*; 2021; 426: 130345.
- Fastier-Wooller JW, Vu T-H, Nguyen H, Nguyen H-Q, Rybachuk M, Zhu Y, Dao DV, Dau VT. Multimodal fibrous static and dynamic tactile sensor. *ACS Appl. Mater. Interfaces*; 2022; 14(23): 27317–27327.